Macromolecules **1994**, *27*, 7415−7422

Molecular Structure by Neutron Scattering of Thermoreversible Gels from Chemically-Modified Poly(vinyl chloride)s[†]

D. Lopez,[‡,⊥] M. Dahmani,[‡] C. Mijangos,[‡,⊥] A. Brûlet,[§] and J.-M. Guenet[*,‡]

Laboratoire d'Ultrasons et de Dynamique des Fluides Complexes, Université Louis Pasteur, CNRS URA 851, 4 rue Blaise Pascal, F-67070 Strasbourg Cedex, France, and Laboratoire Léon Brillouin, CEA−CNRS, CEN Saclay, F-91191 Gif-sur-Yvette Cedex, France

Received June 29, 1994; Revised Manuscript Received September 1, 1994[⊗]

ABSTRACT: The molecular structure of thermoreversible gels made up of poly(vinyl chloride) (PVC) and chemically-modified PVCs in diethyl oxalate has been investigated by small-angle neutron scattering. The chemical modification, which chiefly takes place in the less stereoregular sequences, consists of replacing a few chlorine atoms by either hydrogen or benzothiolate groups. It is shown that small modifications significantly alter the gel structure. At small q vectors the results are analyzed by considering *cross-section polydispersed fibers* characterized by a distribution function of the type $w(r) \sim r^{-1}$. Results at larger q vectors, which yield a q^{-2} behavior, indicate that the fibers are no longer compact at short distances. This behavior is interpreted with a sheetlike structure, which is thought to arise from the formation of a polymer−solvent complex. Fiber associations, which occurs essentially through the *weak links*, is accounted for by an *interdigitation mechanism* of the sheetlike structures. All the results on the different samples are discussed in the light of the polymer−solvent complex and its sheetlike structure and the interdigitation mechanism.

Introduction

The propensity of poly(vinyl chloride) (PVC) solutions to turn into thermoreversible gels is a phenomenon that has been known for over 40 years.[1−3] The reasons why such a heterotactic polymer should give strong gels[3] have always puzzled scientists. Even if the low degree of crystallinity can be resolved by assuming incorporation of isotactic defects into the crystalline lattice, which is predominantly made up of syndiotactic sequences,[4,5] the gel elastic modulus is still paradoxically larger than what can be achieved with model multiblock polymers in which one type of sequence is crystallizable.[6] Clearly, other gel formation mechanisms have to be invented to account for the modulus paradox.

Recently, Najeh et al.[7] have carried out a thorough study of the gel modulus vs gel swelling by using a series of monoesters and diesters. They have concluded on the basis of the fiberlike model[8,9] that the elasticity is of *enthalpic* origin, i.e., existence of rigid, as opposed to flexible, structures. In the case of monoesters, this is achieved by the nonorganized parts being under their glass transition. In the case of diesters, fiber rigidity is obtained through the formation of a polymer−solvent complex,[10] which leads to the creation of some order in what would be otherwise nonorganized domains. This complex is said to occur through electrostatic interaction between the hydrogen on the H−C−Cl bond and the oxygen of the carbonyl on the diester, thereby allowing the diester to bridge different chains.

In this paper we report on a study of the evolution of the gel structure in diethyl oxalate, a complex-forming diester, on chemically-modified PVCs. Several studies have reported the possibility of gradually replacing chlorine atoms by different substituents.[11−14] This substitution leaves the highly syndiotactic sequences virtually unaltered, yet it affects the physical behavior of the gels formed from these chemically-modified PVCs.[13] As the chemical modification can be carried out on a few monomers only, the modified polymer may be regarded as PVC with some defects. The replacement of chlorine atoms will readily alter the polarization of the H−C−Cl bond and ultimately the propensity to produce a polymer−solvent complex as outlined above. This study is also an extension of a former investigation by Abied et al.[9] by means of small-angle neutron scattering of PVC gels in diethyl oxalate.

Experimental Section

Materials. The PVC sample used as a starting material was provided by Rio Rodano Industries, Spain. The number-average molecular weight, determined by osmometric measurements, was found to be $M_n = 3.2 \times 10^4$. Tacticity characterization by ^{13}C-NMR gave the following proportions of triads: syndiotactic = 0.31, heterotactic = 0.5, and isotactic = 0.19.

Sodium benzenethiolate was synthesized from the reaction of sodium with thiophenol as described in earlier articles.[12,14] Lithium aluminum hydride (H_4LiAl) was purchased from Merck and used without further purification.

Tetrahydrofuran (THF) was supplied by Scharlau and distilled prior to use. Cyclohexanone was purchased from Aldrich. Deuterated diethyl oxalate (DEOD) was synthesized from oxalyl chloride and deuterated ethyl alcohol.[15] The deuterated diethyl oxalate was over 99% deuterium labeled.

Chemical Reactions. As mentioned above, the chemical modification allows one to replace gradually chlorine atoms by other atoms or substituents. In this study two types of randomly-modified PVCs were prepared:

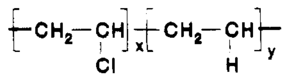

$$\left[\mathrm{CH_2{-}\underset{Cl}{CH}}\right]_x\left[\mathrm{CH_2{-}\underset{H}{CH}}\right]_y$$

VC-E

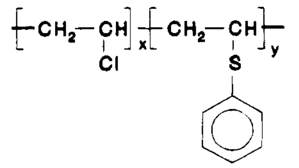

VC-VTB

---

[*] To whom correspondence should be addressed.

[†] This work has been supported by a grant from the EEC (Human Capital and Mobility Program) enabling the creation of a laboratories network entitled "Polymer−solvent organization in relation to chain microstructure".

[‡] Laboratoire d'Ultrasons et de Dynamique des Fluides Complexes.

[§] Laboratoire Léon Brillouin.

[⊥] Permanent address: Instituto de Ciencia y Tecnologia de Polimeros, CSIC, Juan de la Cierva, 3 E-28006 Madrid, Spain.

[⊗] Abstract published in *Advance ACS Abstracts*, November 1, 1994.

0024-9297/94/2227-7415$04.50/0

Table 1. Percent of Conversion and Density As Measured in Cyclohexanone for the Different Samples

sample	% conv	density (g/cm^3)
PVC	0.0	1.415
EPVC2	5.2	1.394
EPVC3	11.1	1.39
SPVC2	1.6	1.398
SPVC3	5.3	1.352
SPVC4	10.0	1.325

In what follows, for simplicity's sake, VC–VTB and VC–E samples will be designated as SPVC and EPVC, respectively.

(1) Substituted PVCs (SPVC). The substitution reactions of PVC with sodium benzenethiolate in the melt using DOP as a plasticizer and stearic acid as a lubricant were performed in a Brabender plasticorder system. As in previous works,[14,15] the reactions were carried out in a single step for different quantities of polymer, nucleophile, and plasticizer. The processing conditions were $T = 160$ °C and 40 rpm. At appropriate reaction times, SPVC samples were drawn out, purified three times with THF–MeOH as the solvent–precipitant system, and dried at 40 °C under vacuum for 2 days.

(2) Reduction of PVCs (EPVC). The reduction reactions of PVC with H_4LiAl as detailed in ref 11 were carried out in a three-necked flask equipped with an inlet tube for nitrogen, reflux condenser, dropping funnel, and Teflon-coated stirring bar. The PVC sample (4.4 g) was dissolved in anhydrous THF (150 mL); after dissolution, H_4LiAl (4.14 g) was added under a steady flow of nitrogen. The mixture was refluxed at 70 °C for different times to prepare copolymers with varying compositions. After the desired reaction time, the mixture was slowly added with vigorous stirring to cold methanol (2 L) so as to recover the polymers by precipitation. Distilled water (2 L) and concentrated hydrochloric acid (25 mL) were added to decompose the excess of H_4LiAl, and the mixture was stirred for 15 h. The EPVC polymer samples were purified three times with THF–MeOH as the solvent–precipitant system and dried at 40 °C under vacuum for 2 days.

Characterization of the Modified Polymers. (1) Chemical Structure. The chemical composition of the SPVC samples was determined by UV spectroscopy using a calibration curve and is given in Table 1.

The chemical composition of the EPVC samples was determined by ^{1}H-NMR spectroscopy. Spectra were obtained at 200 MHz with a Varian XL200 from 5% (w/v) solutions in deuterated nitrobenzene–deuteriochloroform (1:1) at 25 °C. The mole percent of ethylene units can be calculated from conv (%) $= [I(CH_2) - 2I(CH)]/[I(CH_2) + 2I(CH)]$. Resonance areas of the methylene carbons $I(CH_2)$ ranging from 0.6 to 2.8 ppm and those of the methine ones I(CH) ranging from 3.7 to 4.8 ppm were measured with a compensating polar planimeter. Chemical compositions are also reported in Table 1.

(2) Microstructure. The stereochemical structures of both the initial and the modified polymers were determined at 90 °C by ^{13}C-NMR either from solutions in deuterated dioxane (SPVC copolymers) or from solutions in a 1,2-dichlorobenzene–deuterated dioxane mixture (EPVC copolymers) on a 300 MHz XL Varian spectrometer operating at 75.5 MHz and using conditions described elsewhere.[13] The resonances used were those of the CHCl methine carbons of the backbone, ranging from 57 to 62 ppm for SPVC copolymers and from 57 to 67 ppm for EPVC copolymers. The calculations were carried out by measuring the relative areas of the different peaks with a compensating polar planimeter.

It is worth emphasizing here that both types of modification are stereospecific. Modification occurs essentially on the isotactic and heterotactic triads leaving syndiotactic triads virtually unaffected (for further details, see discussion in refs 11 and 13).

(3) Polymer Density. Polymer sample densities were determined in a PAAR/DMA60 densitometer at 22 °C from polymer solutions in cyclohexanone at four different concentrations. Solutions were prepared by dissolving the polymer sample in cyclohexane at 150 °C while stirring. Results are given in Table 1.

Neutron Scattering. (1) Sample Preparation. Solutions were prepared in test tubes by heating at 150 °C a mixture of polymer and DEOD under vigorous stirring until dissolution was completed. The number of monomer units per unit volume was kept constant for all the polymer solutions starting with a 5×10^{-2} g/cm^3 (concentrations in g/cm^3 can be found in figure captions). These solutions were introduced into sealable rectangular quartz cells of optic path 5 mm. The samples were then aged for a minimum of 7 days prior to collecting the neutron data.

(2) Measurements. The experiments were performed at the ORPHEE reactor located at the Laboratoire Léon Brillouin (LLB) (CEN Saclay, France) on the "PAXE" small-angle camera equipped with a two-dimensional sensitive counter (further details are available on request at LLB). The transfer momentun $q = 4\pi/\lambda(\sin\theta/2)$ (λ = neutron wavelength and θ scattering angle) was in the range $10^{-1} \le q\ (\mathrm{nm}^{-1}) \le 2.5$ (for $\lambda = 0.6$ nm).

A mechanical wavelength selector was used to provide a wavelength distribution characterized by $\Delta\lambda/\lambda \simeq 10\%$. The experiments were carried out at 20 ± 1 and 70 ± 1 °C.

As usual, the spectra were corrected for transmission and thickness and were normalized by an incoherent spectrum of hydrogenated *cis*-decalin. The signal scattered by the deuterated solvent was removed from the total scattered intensity to correct for solvent coherent scattering. The hydrogenated polymer incoherent, flat scattering was calculated by a method devised by Fazel et al.[16] and subsequently subtracted. The normalized intensity scattered by the protonated PVC species then reads

$$I_N(q) = KC_H S_H(q) \qquad (1)$$

in which C_H and $S_H(q)$ are the concentration and the scattering function of the hydrogenated polymer chains, respectively, and K is a constant:

$$K = \frac{4\pi\delta N_A T_{dec}(a_H - na_D)^2}{g(\lambda) m_0^{\,2}(1 - T_{dec})} \qquad (2)$$

in which N_A is Avogadro's number, m_0 is the monomer molecular weight, T_{dec} and δ are the *cis*-decalin sample transmission and thickness, respectively, a_H and a_D are the scattering amplitudes of the polymer species and of the solvent, respectively, and $n = d_D m_{0H}/d_H m_{0D}$, in which d_D and d_H are the densities of the solvent and of the monomer and m_D is the solvent molecular weight. $g(\lambda)$ is a corrective term which depends upon the neutron wavelength, the wavelength distribution, and the camera. This parameter was determined by Cotton's method.[17]

The absolute intensity, $I_A(q)$, is then simply

$$I_A(q) = I_N(q)/K \qquad (3)$$

The scattering amplitude occurring in the constant K was calculated for the modified PVCs on the basis of a random copolymer structure. This is not strictly correct as the less stereoregular sequences were more chemically altered than the syndiotactic ones.[11,13] Still, as the degree of chemical modification was kept low, the values of K do not differ significantly from one sample to another (the maximum variation is about 15%). Consequently, values deduced from $I_A(q)$, such as masses per unit length or per unit area, can be regarded as good approximations despite that they are, strictly speaking, apparent ones due to the block character of the modified polymers.

Results and Discussion

We shall first discuss the results obtained on the original PVC sample on the basis of fiberlike models developed by Abied et al.[9] As in the investigation presented herein the q range has been extended, additional information has been deduced by a theoretical derivation carried out by Guenet.[18] The results gathered on the modified PVCs will be examined afterward.

PVC/Diethyl Oxalate Gels. Before proceeding further, it is worth summarizing Abied et al.'s approach and conclusions on PVC aggregates and gels in diethyl oxalate.[9]

Depending on the ageing time, two typical scattering curves are obtained:

(i) For *a nascent system*, Abied et al. identified two domains on either side of a scattering vector $\tilde{\mathbf{q}}$: at low scattering vectors $I(q) \sim q^{-4}$ while at large scattering vectors $I(q) \sim q^{-2}$.

(ii) For *systems aged for a minimum of 24 h*, the large q scattering curve remained unchanged while at low q, $I(q) \sim q^{-n}$ with $n > 4$.

These authors interpreted the scattering curves by means of a fiberlike structure on the basis of electron microscopy micrographs by Yang and Geil.[8] In this framework, for *nascent systems*, they considered the aggregates to be made up of independent fiberlike structures, comparable to solid cylinders of infinite length. Accordingly, the q^{-4} behavior corresponded to the so-called Porod regime. The q^{-2} behavior is, however, not expected for compact objects. Abied et al.[9] concluded that below some distance defined by $\tilde{\mathbf{q}}$ the fibers were no longer compact. They further concluded that this was an indication of the existence of a polymer–solvent complex. They, however, dwelt upon the fact that, due to the short q range in which the q^{-2} behavior was seen, the exponent 2 might as well be an apparent exponent. They insisted that this range had to be extended so as to find out whether a q^{-1} behavior could be observed which would indicate the presence of fairly rigid PVC chains separated by intercalated solvent molecules. Schematically speaking, these authors described the fibers as consisting of three domains: *well-organized domains with no solvent occluded* wherein predominantly syndiotactic chain portions form classical PVC crystals, *polymer–solvent organized domains* wherein less stereoregular chain portions form a complex with solvent molecules, and *disordered domains*.

For *aged systems* they accounted for the existence of an exponent larger than 4 by considering fibers associations through the so-called *weak links* (PVC–solvent complex). As a matter of fact, a purely power law decay with exponents larger than 4 cannot exist. So exponents larger than 4 are *apparent exponents* arising from the existence of terms of higher orders in the development of the scattering factor. In the case of cylinders the scattering function contains terms of order higher than 4:[19]

$$I_{\infty}(q) \sim \frac{\mu_{\mathrm{L}}}{q^4 r^3}\left[1 + \frac{3}{8q^2r^2} + \ldots\right] \tag{4}$$

These q^{-6} terms are usually negligible except for two cases: very small cross-sectional radius or connections between cylinders. Abied et al. chose the latter explanation. As will be discovered in what follows, this hypothesis will receive further confirmation.

As these associations disappeared by simply heating at 60 °C, Abied et al. concluded that fiber association proceeded chiefly through the *weak links*, that is through the formation of the PVC/diethyl oxalate complex.

Finally, they showed that, once properly normalized by the polymer concentration, the scattering curves of *aged* 2% aggregates or 15% gel were identical. This clearly indicated that a *large part of the junctions arose from the formation of the PVC/diethyl oxalate complex.*

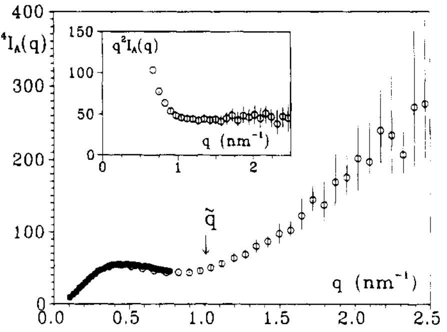

Figure 1. Intensity scattered by a 5% PVC/DEO gel at 20 °C ($q^4I(q)$ vs q representation). Full and open circles stand for different sample–detector distances. Inset: the same intensity plotted by means of a Kratky plot ($q^2I(q)$ vs q).

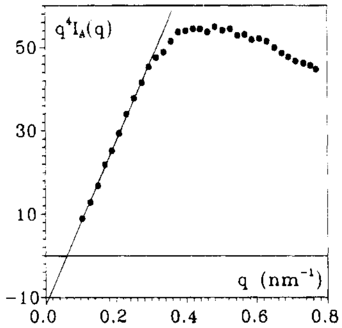

Figure 2. Intensity scattered in the low-angle domain by a 5% PVC/DEO gel at 20 °C ($q^4I(q)$ vs q representation). The straight line defines the *transitional q range*. The intercept of this line with the q axis gives $r_{\max}$.

Results reported in Figure 1 for a 5% gel in DEO plotted by means of a $q^4I_A(q)$ vs q representation confirm Abied et al.'s findings. One can clearly separate two domains below and above $\tilde{\mathbf{q}}$.

Above $\tilde{\mathbf{q}}$ the exponent 2 is confirmed in a large q range as highlighted in the inset of Figure 1 by means of a $q^2I_A(q)$ vs q representation.

Below $\tilde{\mathbf{q}}$ the q^{-n} behavior with $n > 4$ can be seen but, in addition, at smaller angles (designated as a *transitional q range* in Guenet's theoretical derivation[18]) the $q^4I_A(q)$ representation brings out another behavior of the type (Figure 2)

$$q^4 I_{\mathrm{A}}(q) \sim aq - b \tag{5}$$

As is detailed in ref 18, this behavior can be simply accounted for by considering a population of fibers with different cross-section radii characterized by a continuous weight distribution function $w(r) \sim r^{-1}$ with two cutoff radii, $r_{\min}$ and $r_{\max}$. The intensity in this q range then reads

$$\frac{q^4 I_{\mathrm{A}}(q)}{C} = \frac{2\pi^2 \varrho q - 4\pi\varrho/r_{\max}}{\log(r_{\max}/r_{\min})} \tag{6}$$

in which ϱ is the PVC molecular density (in g mol^{-1} nm^{-3}) and C is its concentration (in g/cm^3).

Accordingly, $r_{\max}$ can be determined from the scattering vector q_0 obtained from the intersection of the scattering curve in the transitional q range with the q axis through the following relation:

$$r_{\max} = \frac{2}{\pi q_0} \simeq \frac{0.637}{q_0} \tag{7}$$

The value of r_{max} is found to be about 11 nm, a figure which is in agreement with Yang and Geil's findings by electron microscopy.[8]

Once r_{max} is determined, r_{min}, the number-averaged cross-section radius r_n, the radius polydispersity $I_p = r_w/r_n$ (r_w = weight-averaged cross-section radius), and ϱ can be obtained straightforwardly from the following quantities obtained from a $q^4I(q)$ vs q representation:

The slope of the intensity in the transitional q range is

$$\sigma = \frac{q^4 I_A(q = Q) - q^4 I_A(q = 0)}{2\pi^2 C Q} = \frac{\varrho}{\log(r_{max}/r_{min})} \tag{8}$$

The ordinate of the plateau *in the Porod range* is

$$\sigma_0 = \frac{q^4 I_A(q)}{4\pi C} = \frac{\varrho}{r_n} \tag{9}$$

r_{min} is then simply derived from

$$\frac{r_{max}}{r_{min}} = \frac{\sigma_0 r_{max}}{\sigma} + 1 \tag{10}$$

r_{min} is found to be about 2 nm. Knowledge of r_{min} allows us to show that the presence of q^{-6} terms does not arise from the existence of small radii. Under the present theoretical approach the intensity in the onset of the Porod range is written

$$\frac{q^4 I_A(q)}{C} = \frac{4\pi\varrho}{r_n} + \frac{1}{q^2 r_{min}^3 \log(r_{max}/r_{min})} \tag{11}$$

As can be seen, the q^{-6} term is virtually negligible for r_{min} = 2 nm and is thus not liable to give rise to a noticeable excess scattering. This gives further support to Abied et al.'s hypothesis that relates the experimental excess scattering to the existence of connections between fibers. The number-averaged radius, r_n, and the weight-averaged radius are obtained from

$$\frac{1}{r_n} = \frac{1/r_{min} - 1/r_{max}}{\log(r_{max}/r_{min})} \tag{12}$$

$$r_w = (r_{max} - r_{min}) \times \log^{-1}(r_{max}/r_{min}) \tag{13}$$

The ratio between r_{min} and r_{max} is found to be about 5, which gives a polydispersity of about $r_w/r_n \approx 1.2$. The PVC molecular density, ϱ = 310 g mol^{-1} nm^{-3}, turns out to be much lower than what is calculated on the basis of the PVC crystalline lattice, i.e., 931 g mol^{-1} nm^{-3}.[20] This result is in agreement with the hypothesis of a PVC/diethyl oxalate compound: intercalating solvent molecules between PVC chains must entail a marked decrease of the PVC molecular density. It is worth emphasizing that the present theoretical analysis permits direct determination of ϱ whereas in Abied et al.'s paper these authors could only surmise a lower density but were not able to derive any experimental value.

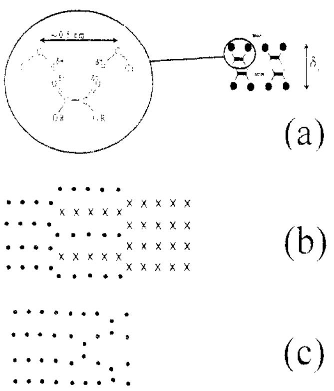

Figure 3. Schematic molecular structure: (a) representation of the DEO–PVC interaction and the resulting sheetlike arrangement. The chains (●) are seen parallel to their axis. (b) Sketch of how two fibers may interpenetrate by an *interdigitation mechanism*. The black circles and crosses indicate chains belonging to two different fibers. Again the chains are seen parallel to their axis. (c) Illustration of the formation of bottlenecks.

This result is further consistent with the q^{-2} behavior beyond $\tilde{\mathbf{q}}$, which is believed to arise from PVC chains separation. The q^{-2} behavior seen in the large q range suggests the existence of a sheetlike organization as opposed to fairly rigid PVC chains spaced apart from one another. In the latter case, a q^{-1} behavior (or at least an exponent smaller than 2) would be expected instead. Indeed, infinitely thin sheets scatter as[21]

$$I(q) \sim 2\pi\mu_s/q^2 \tag{14}$$

in which μ_s is the mass per unit area of the sheet. This behavior is reached for a scattering vector $\tilde{\mathbf{q}}$ such as $\tilde{\mathbf{q}} = f/\delta_s$, wherein δ_s is the distance between sheets and f is a constant factor. Usually f is somewhere between 1 and 2, which presently gives $1.0 \le \delta_s \le 2.0$ nm. Again, this result is consistent with the low value found for the PVC molecular density. Preliminary X-ray investigations on a 15% gel have revealed a broad reflection at 0.74 nm, which is most probably related to the sheet spacing.

Provided the interpretation by means of sheet structures proves to be correct, the PVC/DEO complex resembles PEO/dihalogenobenzene complexes[22] and the so-called *p-phase* in iPS/*cis*-decalin compounds.[23] Possibly, sheetlike structures may be quite a common feature for the molecular organization of polymer–solvent complexes.

Although we cannot claim it for sure, it is most probable that the PVC chains take on an extended conformation in the sheet structures. In Figure 3a is portrayed a possible sheetlike structure involving the solvent molecules. Here, the interaction $C{=}O^{\delta-}\cdots{}^{\delta+}H{-}C{-}Cl$ is again considered.[7,9,24,25] We further surmise that the formation of *weak links* between two different fibrils via the complex occurs through *interdigitation* as pictured in Figure 3b.

Interestingly, μ_s can be calculated from relation 14. One finds μ_s = 145 ± 15 g mol^{-1} nm^{-2}. It is worth comparing this value to those of the denser planes in the crystalline lattice of syndiotactic PVC crystals:[20] in the 200 plane $\mu_{s200} \approx$ 470 g mol^{-1} nm^{-2}, in the 010 plane $\mu_{s010} \approx$ 450 g mol^{-1} nm^{-2}. Two cases are worth contemplating to account for this discrepancy:

(i) The distance between PVC chains located in the same sheet is larger than what can be achieved in syndiotactic PVC crystals. This hypothesis seems rather unlikely on the basis of the molecular model drawn in Figure 3a. Besides, if this distance were too large, then one would end up with well-separated PVC chains and, accordingly, another intensity behavior.

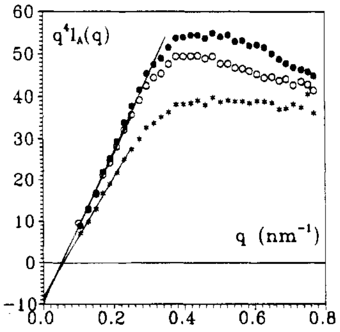

Figure 4. Intensity scattered in the low-angle domain by a 5% EPVC/DEO system at 20 °C ($q^4I(q)$ vs q representation): (●) PVC; (○) EPVC2; (*) EPVC3.

(ii) The fibers are said to be composed of parts made up with PVC/diethyl oxalate complex, on the one hand, and PVC "crystals" with sequences of highest syndiotacticity, on the other hand.[9] The latter should scatter as q^{-4} in all the q range investigated. Schematically speaking, the intensity can then be written in this q range:

$$I(q) \sim X^2q^{-2} + (1-X)^2q^{-4} + ... \qquad (15)$$

in which X is the proportion of complex and $1 - X$ that of "syndiotactic crystals". At high **q** vectors the q^{-2} term will dominate the scattering whence the intensity scattered by the sheets will be reduced by a factor X. To obtain $\mu_s \approx 450$ g mol^{-1} nm^{-3}, one has to take $X \approx 0.57$. This simplistic analysis through relation 15 provides a lower limit for the amount of PVC/DEO complex in the gel. The actual amount of PVC/DEO complex is, however, likely to be larger as one does not expect a large proportion of "syndiotactic crystals". The highest estimates, which consider "syndiotactic crystals" containing defects of stereoregularity, amount to about 10%.[4,5] A more refined analysis should also take into consideration intermediate amorphous domains that may contain some occluded solvent molecules but without sheetlike organization.

It should also be emphasized that in DSC investigations the melting of the *weak links* gives an endotherm far more salient that the melting of the *strong links*. This is consistent with the figure derived from the above analysis.

Modified PVC/Diethyl Oxalate Gels and Aggregates. As above, we shall discuss the results for $\mathbf{q} < \tilde{\mathbf{q}}$ and for $\mathbf{q} > \tilde{\mathbf{q}}$. For each system the results obtained for $\mathbf{q} < \tilde{\mathbf{q}}$ will be plotted by means of a $q^4I_A(q)$ vs q representation, while for $\mathbf{q} > \tilde{\mathbf{q}}$ a Kratky plot ($q^2I_A(q)$ vs q) will be used. We shall present first the data on EPVC systems and then those on SPVC systems.

(1) EPVC Gels and Aggregates at 20 °C. Replacing chlorine by hydrogen atoms has directly visible consequences: *the most modified sample (EPVC3, 11.1% chlorine atoms replaced) forms no macroscopic gel at a 5% concentration.*

Table 2. Different Parameters for the Fibrils Constituting the PVC Gels or Aggregates[a]

sample	r_{max} (nm)	r_{min} (nm)	r_n (nm)	I_p	ϱ (g mol^{-1} nm^{-3})
PVC	10.6 *[11.3]*	2.2 *[1.8]*	4.4 *[3.9]*	1.21 *[1.34]*	318 *[220]*
EPVC2	12.0 *[13.0]*	2.1 *[2.0]*	4.5 *[4.4]*	1.27 *[1.31]*	297 *[180]*
EVPC3	11.3 *[11.3]*	1.95 *[1.7]*	4.1 *[3.8]*	1.29 *[1.3]*	260 *[110]*
SPVC2	9.8 *[10.6]*	1.8 *[1.9]*	3.7 *[4.0]*	1.27 *[1.26]*	272 *[178]*
SPVC3	9.8 *[8.0]*	1.8 *[1.7]*	3.7 *[3.3]*	1.27 *[1.23]*	237 *[117]*
SPVC4	9.5	1.5	3.2	1.35	180

[a] Bracketed figures in italics stand for those data collected at 70 °C.

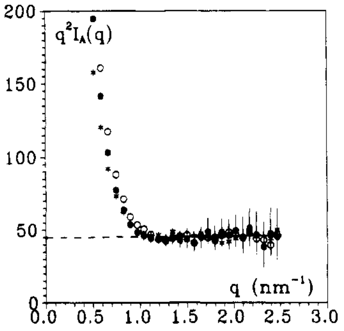

Figure 5. Intensity scattered in the high-angle domain by a 5% EPVC/DEO system at 20 °C (Kratky plot, $q^2I(q)$ vs q representation): (●) PVC; (○) EPVC2; (*) EPVC3.

Neutron results in Figure 4 obtained for $\mathbf{q} < \tilde{\mathbf{q}}$ also present noticeable change. While at low q the $(aq - b)$ behavior is still observed, at high q the scattered intensity tends to the pure q^{-4} behavior (gradual disappearance of the excess scattering at the onset of the Porod range). Analysis performed in the *transitional domain* indicates no noticeable alteration of r_{max}, r_{min}, and r_n (see Table 2). These two observations are again consistent with the hypothesis that attributes the q^{-6} terms to fiber connections through the *weak links*. The fact that the EPVC3 sample forms no gel is consistent with this view. As will be seen below from experiments carried out at 70 °C, the vanishing of the q^{-6} terms is also directly related to the disappearance of the weak links.

We further note that the PVC molecular density ϱ decreases, but not dramatically. Between PVC and EPVC3 samples, the change is but about 18% (see Table 2). This might indicate a slight swelling of the sheetlike domains, i.e., a slightly larger spacing between the sheets.

Results obtained for $\mathbf{q} > \tilde{\mathbf{q}}$ are plotted in Figure 5. As can be seen, there is viturally no difference between the three samples, which is consistent with a virtually constant spacing between sheets. This rather suggests that the accuracy in determining ϱ is about 15–20%. This may stem from the calibration procedure, which is entirely dependent upon the proper calculation of the scattering amplitude of the samples. As already emphasized, this parameter is slightly misevaluated as the modified PVCs have been purposefully approximated to random copolymers.

The molecular interpretation of these results together with their conclusions can again make use of the PVC/DEO complex. Whenever a chlorine atom is replaced by a hydrogen atom, a positive fractional charge vanishes on the chain, and correspondingly, a C=O⋯H interaction disappears. The gradual disappearance of weak links is conclusively linked to the polarization of H–C–Cl. What takes place in the sheetlike domains can be viewed as the formation of bottlenecks due to the "polyethylene-like" interaction between parts devoid of chlorine atoms (see Figure 3c); the presence of only a few such bottlenecks is liable to hinder very efficiently the interdigitation process which we believe to be responsible for the formation of weak links between fibers. It is worth emphasizing that the formation of these bottlenecks is supposed not to affect significantly

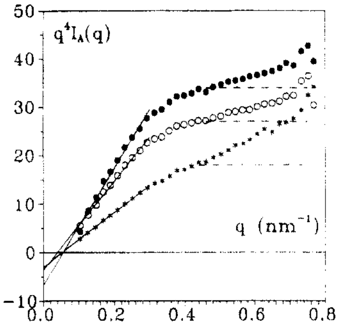

Figure 6. Intensity scattered in the low-angle domain by a 5% EPVC/DEO system at 70 °C ($q^4I(q)$ vs q representation): (●) PVC; (○) EPVC2; (*) EPVC3. The dashed lines stand for the estimated Porod asymptotic regime.

the sheet spacing, which is consistent with the results obtained for $\mathbf{q} > \tilde{\mathbf{q}}$.

(2) EPVC Gels and Aggregates at 70 °C. At T = 70 °C, for 5% concentrated systems no macroscopic gel exists, even for the unmodified PVC. Under these conditions, all the samples are above the weak links melting temperature (50 < T_m < 60 °C for PVC in DEO[10]). Yet, aggregates remain that are, manifestly, swollen as indicated by the rapid departure from the q^{-4} behavior (which is barely visible) and the subsequent decrease of ϱ (see Table 2 and Figure 6). Such a decrease, which by no means can be here attributed to inappropriate calibration, implies that PVC chains are further apart on account of the presence of an excess of solvent molecules. This happens after the melting of the weak links and therefore corresponds to the melting of the PVC/complex. The unquestionable decrease of ϱ for all the EPVC samples, including the unmodified PVC sample, is clearly associated with the disappearance of the weak links, which is consistent with the *interdigitation mechanism*.

Again, there is no marked alteration of r_{max}, r_{min}, and r_n. Swelling should tend to shift the entire distribution toward higher cross-sectional radii. Now, fibers possessing radii larger than 12 nm may be unstable; hence the swelling may be compensated for by a lower number of chains per fibril to achieve the stablest system. For instance, a high-radius fiber may break up into two smaller ones. Here, one may wonder whether the weak links melting releases free chains. As the fibers are supposed to vanish definitively with the melting of the "highly syndiotactic" parts, whose melting occurs well above 70 °C, one may surmise that virtually no or a minimum of free chains should be present. If free chains were, however, present to a large extent, their scattering should rapidly dominate. As a result, a parabolic variation should be ssen all along,[9] which is not the case. Effects arising from free chains can be ignored to a first approximation.

Results obtained for $\mathbf{q} > \tilde{\mathbf{q}}$ (Figure 7) indicate a significant deviation from the q^{-2} behavior, which suggests the breaking up of the sheetlike structure. The present behavior can be interpreted in the framework of parallel rods (PVC extended chains of cross-sectional radius r_c) spaced apart by a distance δ. Such an arrangement of rods scatters, for $q\delta > 1$, as[26]

$$q^2I(q) = \pi\mu_L q \exp(-q^2r_c^2/4)[1 - 2\pi n_A q^{-0.5} f(r)] \qquad (16)$$

in which n_A is the number of extended PVC chains per unit area and $f(r)$ is an oscillating function. If $qr_c \ll 1$ then the exponential term is close to unity, thus allowing one to evaluate μ_L from the initial slope. We find μ_L = 100 ± 10 g mol^{-1} nm^{-1}, a value to be compared to the mass per unit length of PVC μ_{LPVC} = 245 g mol^{-1} nm^{-1}. If we consider the same explanation as used above for the low value of μ_s and assume that only the chains belonging formerly to the complexed domain can take on this extended conformation, then the intensity is written

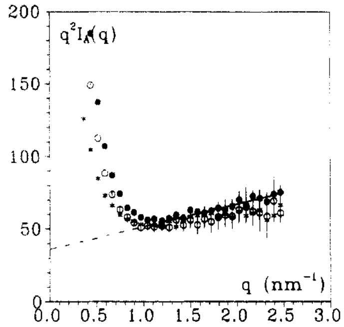

Figure 7. Intensity scattered in the high-angle domain by a 5% EPVC/DEO system at 70 °C (Kratky plot, $q^2I(q)$ vs q representation): (●) PVC; (○) EPVC2; (*) EPVC3.

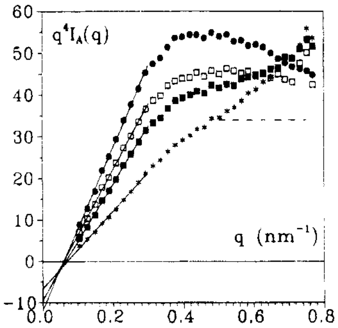

Figure 8. Intensity scattered in the low-angle domain by a 5% SPVC/DEO system at 20 °C ($q^4I(q)$ vs q representation): (●) PVC; (□) SPVC2; (■) SPVC3; (*) SPVC4.

$$I(q) \sim X^2q^{-1} + (1 - X)^2q^{-4} + ... \qquad (17)$$

This provides one with an amount of about 64% for the complexed domain. The fact that the straight line does not go through zero for q = 0 reveals the presence of q^{-2} terms, which is a possible indication of the existence of totally disordered domains as was already suggested above. The figure of 64% is close to that found previously at room temperature from the sheetlike behavior. The analysis in this q range is therefore self-consistent.

(3) SPVC Gels and Aggregates at 20 °C. As with EPVC samples, replacing chlorine atoms by the benzenethiolate groups has a noticeable macroscopic effect: the 5.3% substituted sample gives a very weak gel, and the 10% substituted sample no gel at all. Also, it is worth mentioning that a 100% substituted sample dissolves readily in DEO, which hints at a strong interaction of this solvent with the benzenethiolate group.

This kinds of substitution alters readily the scattering curves as there is a noticeable discrepancy between the unmodified PVC and the 1.6% modified SPVC sample for $\mathbf{q} < \tilde{\mathbf{q}}$ (Figure 8). Again, all the results can be analyzed in the *transitional q range* with the same theoretical approach used above. Data are gathered in Table 2. As a rule, r_{max} and r_{min} are noticeably lower than with EPVC samples. Also, the molecular density decreases quite significantly and more rapidly than for

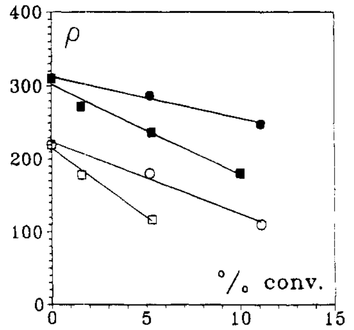

Figure 9. Variation of the experimental value of ϱ as a function of the degree of conversion. Circles stand for EPVC (full at 20 °C and open at 70 °C) while squares stand for SPVC (full at 20 °C and open at 70 °C).

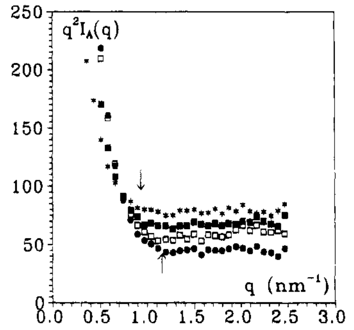

Figure 10. Intensity scattered in the high-angle domain by a 5% SPVC/DEO system at 20 °C (Kratky plot, $q^2I(q)$ vs q representation): (●) PVC; (□) SPVC2; (■) SPVC3; (*) SPVC4. Arrows highlight where the q^{-2} behavior is reached.

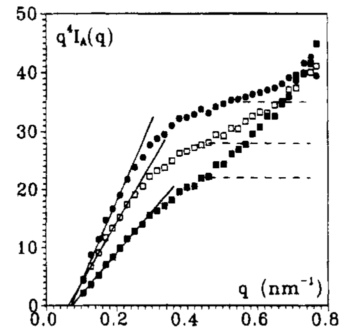

Figure 11. Intensity scattered in the low-angle domain by a 5% SPVC/DEO system at 70 °C ($q^4I(q)$ vs q representation): (●) PVC; (□) SPVC2; (■) SPVC3. The dashed lines stand for the estimated asymptote in the Porod regime.

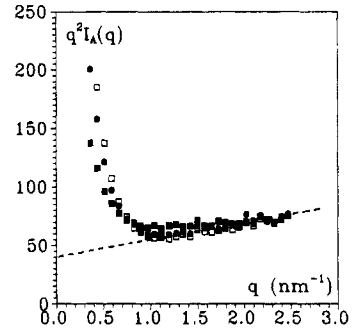

Figure 12. Intensity scattered in the high-angle domain by a 5% SPVC/DEO system at 70 °C (Kratky plot, $q^2I(q)$ vs q representation): (●) PVC; (□) SPVC2; (■) SPVC3.

EPVC sample (for comparison, see Figure 9). Similarly, the q^{-6} terms vanish more rapidly as they are virtually negligible for the 1.6% substituted sample. All these results show that substitution by benzenethiolate groups entails a rapid swelling of the complexed parts of the aggregates and, correspondingly, disappearance of the connections between fibers. This is consistent with what is observed at the macroscopic level.

For $\mathbf{q} > \tilde{\mathbf{q}}$ (Figure 10) SPVC gels and aggregates are at variance with EPVC samples on two items: (i) the q^{-2} behavior is reached for smaller q and (ii) the level of intensity increases with increasing degree of substitution.

The decrease of $\tilde{\mathbf{q}}$, which suggests an increase in the spacing between sheets, is consistent with the significant decrease of the molecular density.

The increase of the intensity level ought to be examined bearing in mind that, all things being constant, the mass per unit area must increase with increasing degree of substitution as a benzenethiolate group is heavier than a chlorine atom. Yet, this increase should be of about 12% for the most substituted sample (provided the interchain distance remains unaltered) whereas it actually is of about 70%. Again, the misevaluation of the contrast factor may be responsible for this discrepancy. Another possibility worth contemplating is a decrease of the interchain distance within a same sheet, which would augment the mass per unit area. We shall leave this point as an open question with the presently available data.

Manifestly, benzenethiolate substitution entails bigger effects than H substitution. This may stem from the fact that this chemical group is far larger than a chlorine atom, thus entailing steric effects, but also that this type of substitution improves the polymer–solvent interaction (see above), which thereby produces a swelling that is liable to hamper the interdigitation mechanism.

(4) SPVC Gels and Aggregates at 70 °C. As with EPVC samples, the macroscopic gel is molten. This again shows that the weak links have been melted.

For $\mathbf{q} < \tilde{\mathbf{q}}$ the same effect as observed for EPVC samples is observed (Figure 11): the q^{-4} behavior is barely visible. Applying the same theoretical analysis as above shows little change in the different values of cross-sectional radii. Conversely, as expected, the PVC molecular density decreases quite markedly. Figure 9 highlights the more pronounced decrease of this parameter for SPVC samples than for EPVC samples.

For $\mathbf{q} > \tilde{\mathbf{q}}$ the 1.6% substituted sample displays close similarity to the unmodified PVC system, namely, a rodlike behavior. Conversely, the 5.3% substituted sample seems to obey a q^{-2} behavior instead. Possibly, the chains take on a Gaussian conformation, at least locally, rather than a near-extended structure. At any rate, the results in this range are again consistent with the values calculated for the PVC molecular density.

Concluding Remarks

There are several outcomes from the results presented here. Three of them are worth emphasizing and briefly discussing.

The fiberlike gel structure receives additional support. It is further shown by means of Guenet's theoretical derivation that these fibers are characterized by a cross-sectional radius distribution of the type $w(r) \sim r^{-1}$. The different radii derived from this theoretical analysis are consistent with those deduced from other techniques.[8] It remains now to understand why the fibers' growth produces such a distribution law.

The q^{-2} behavior at large angles has led us to put forward the sheetlike model together with the interdigitation mechanism to account for the formation of the weak links. Preliminary X-ray diffraction data are consistent with the sheetlike structure. It is now necessary to test the validity of the interdigitation mechanism.

The body of experimental data shows clearly that the formation of weak links takes place in the less stereoregular domains keeping in mind that the chemical modification is stereospecific. One unambiguously observes the gradual disappearance of these weak links with increasing degree of modification. If only the highly syndiotactic sequences were responsible for the formation of the physical links, then the chemical modification would have had no effect. Similarly, the disappearance of the weak links is conclusively linked to the polarization of the H–C–Cl bond, which gives support to the existence of a PVC–DEO complex occurring in the less stereoregular portions. Interestingly, the replacement of the chlorine atom by a hydrogen or a benzothiolate group entails different effects. H substitution suppresses the bond polarization. The disappearance of weak link, is thought to arise from "bottlenecks" between sheets belonging to the same fiber. Conversely, benzenethiolate substitution does not necessarily preclude the bond polarization, yet the interaction between DEO and this group seems so strong that swelling occurs, which eventually renders the interdigitation inefficient.

Acknowledgment. C.M. is grateful to the Dirección General de Investigación Cientifica y Técnica (DGICYT) for financial support.

References and Notes

(1) Stein, R. S.; Tobolsky, A. V. *Text. Res. J.* **1949**, *18*, 302.

(2) Alfrey, T.; Wiederhorn, N.; Stein, R. S.; Tobolsky, A. V. *Ind. Eng. Chem.* **1949**, *41*, 701.

(3) Walter, A. T. *J. Polym. Sci.* **1954**, *13*, 207.

(4) Juijn, J. A.; Gisolf, A.; de Jong, W. A. *Kolloid Z. Z. Polym.* **1973**, *251*, 456.

(5) Hobson, J.; Windle, A. H. *Makromol. Chem. Theory Simul.* **1993**, *2*, 257.

(6) He, X.; Herz, J.; Guenet, J. M. *Macromolecules* **1988**, *21*, 1757.

(7) Najeh, M.; Munch, J. P.; Guenet, J. M. *Macromolecules* **1992**, *25*, 7018.

(8) Yang, Y. C.; Geil, P. H. *J. Macromol. Sci.* **1983**, *B22* (3), 463.

(9) Abied, H.; Brûlet, A.; Guenet, J. M. *Colloid Polym. Sci.* **1990**, *268*, 403.

(10) Mutin, P. H.; Guenet, J. M. *Macromolecules* **1989**, *22*, 843.

(11) Pourahmady, N.; Bak, P. I.; Kinsey, R. A. *J. Macromol. Sci.* **1992**, *A29* (11), 959.

(12) Lopez, D.; Mijangos, C. *Colloid Polym. Sci.* **1994**, *272*, 159.

(13) Mijangos, C.; Lopez, D.; Muñoz, M. E.; Santamaria, A. *Macromolecules* **1993**, *26*, 5693.

(14) Mijangos, C.; Gomez-Elvira, J. M.; Martinez, G.; Millàn, G. *J. Appl. Polym. Sci.* **1989**, *38*, 1085.

(15) This solvent was synthesized by C. Galin from the Institut Charles Sadron, Strasbourg, France.

(16) Fazel, N.; Brûlet, A.; Guenet, J. M. *Macromolecules* **1994**, *27*, 3836.

(17) Cotton, J. P. In *Neutron, X-ray and Light Scattering*; Lindner, P., Zemb, T., Eds.; Elsevier: Amsterdam, 1991.

(18) Guenet, J. M. *J. Phys. II* **1994**, *4*, 1077.

(19) Kirste, R.; Porod, G. *Kolloid Z. Z. Polym.* **1962**, *184*, 1.

(20) Wilkes, C. E.; Folt, V.; Krimm, S. *Macromolecules* **1973**, *6*, 235.

(21) Porod, G. *Kolloid Z.* **1951**, *124*, 83.

(22) Point, J. J.; Coutelier, C. *J. Polym. Sci., Polym. Phys. Ed.* **1985**, *23*, 231.

(23) Guenet, J. M.; Menelle, A.; Schaffhauser, V.; Terech, P.; Thierry, A. *Colloid Polym. Sci.* **1994**, *272*. 36.

(24) Tabb, D. L.; Koenig, J. L. *Macromolecules* **1975**, *8*, 929.

(25) Monteiro, E. E. C.; Mano, E. B. *J. Polym. Sci., Polym. Phys. Ed.* **1984**, *22*, 533.

(26) Oster, G.; Riley, D. P. *Acta Crystallogr.* **1952**, *5*, 272.